Colloid Polym Sci (2004) 282: 1242–1246
DOI 10.1007/s00396-004-1074-7

ORIGINAL CONTRIBUTION

Susanne Hacke
Dietmar Möbius

Influence of active sites distribution on $CaCO_3$ formation under model biofilms at the air/water interface

Received: 2 December 2003
Accepted: 22 January 2004
Published online: 19 March 2004

S. Hacke
GZG-Kristallographie,
Georg-August-Universität,
Goldschmidtstraße 1, 37077 Göttingen,
Germany

D. Möbius (✉)
Max Planck Institut für Biophysikalische
Chemie, Am Faßberg 11,
37077 Göttingen,
Germany
E-mail: dmoebiu@gwdg.de

Abstract In an approach to understand the influence of structural parameters of interfaces on calcification in biomineralisation, the distribution of COOH groups as active sites in an inert matrix was varied using two-component lipid model monolayers. Octadecanoic acid (ODA) and octadecyl succinic acid (OSA), respectively, were the active components, and methyl octadecanoate (MOD) the inactive matrix. Surface pressure-area isotherms provide evidence for a different distribution of the active components in the matrix. Formation of solid calcium carbonate ($CaCO_3$) with two-component monolayers on subphases containing aqueous $CaCO_3$ was observed in situ by Brewster angle microscopy, where $CaCO_3$ domains appear bright. Striking differences in kinetics and extent of $CaCO_3$ formation were observed between monolayers containing ODA and those containing OSA of the same average surface density of COOH groups.

Keywords Two-component model monolayers · In situ Brewster angle microscopy · Calcium carbonate formation · Kinetics · Critical cluster

Introduction

The formation of solid calcium carbonate ($CaCO_3$) is an important process in biological systems at the interface between living organisms and mineral phases [1, 2, 3,4]. In recent years much effort has been devoted to the characterisation of the extracellular polymeric substances (EPS) in microbial biofilms, which are playing an important role in binding Ca ions in calcification of marine stromatolites [5]. A variety of organised organic matrices as templates has been developed for controlling the nucleation and growth of solid $CaCO_3$. Insoluble Langmuir monolayers at the air-water interface provide excellent opportunities to systematically vary relevant parameters. Therefore, lipid monolayers with different head groups have been used for such investigations [6,7]. The transfer of structural information from the monolayer to the 3-D crystal can also provide evidence on the correlation between size and structure of the 2-D nuclei and the tendency for the 3-D crystal formation. The minimal lateral size of monolayer domains inducing 3-D crystal nucleation may be determined by using mixed Langmuir films. In an attempt to mimic the dimensions of crystalline material, mixed monolayers of a long-chain amide and of a particular amphiphilic acid have been used for epitaxial growth of 3-D crystals of silver propionate [8,9]. In this two-component monolayer, the amide is inactive, and by variation of the molar ratio of the two components, it has been shown that domains of the active component of finite size are required to initiate crystallisation of silver propionate [8].

A new approach in the investigation of $CaCO_3$ formation at interfaces is the variation of parameters like density and distribution of active sites in an inert matrix with respect to initialisation of mineralisation, in order to obtain new insights into the nucleation process as well as to control the size of the crystal

nuclei. As active site we used the carboxyl group COOH [lipids: octadecanoic acid (ODA) and octadecyl succinic acid (OSA)]. The methyl carboxylate group [lipid: methyl octadecanoate (MOD)] served as inactive matrix for the variation of the average surface density of the active groups. For a variation of the distribution, the dicarboxylic acid OSA was used to intentionally provide a pair of active groups in close vicinity to each other. Since the pure monolayers of both ODA and OSA did show limited long-term stability on aqueous solutions of $CaCO_3$, the formation of solid $CaCO_3$ with the two-component monolayers only are reported here. Brewster angle microscopy (BAM) allows the observation of the topography of monolayers and temporal changes, e.g. during compression, at the air-water interface without the addition of a fluorescent probe [10, 11,12]. BAM has been used for studying in situ the interfacial growth of meso-structured silica thin films in the presence of water-soluble tensides [13], and the $CaCO_3$ precipitation in dependence on long chain fatty acids of various chain length [14]. The formation of solid $CaCO_3$ initiated by the active head groups of a two-component monolayer should also be detectable in situ with a Brewster angle microscope if the domains are of sufficient lateral size, since a layer of $CaCO_3$ a few nanometres thick has a reflectivity similar to that of the monolayer at the air-water interface [15].

Materials and methods

Materials ODA and MOD were purchased from Merck (Germany). OSA was purchased from Lancaster Synthesis, England. All lipids were used without further purification and dissolved in chloroform (Baker, HPLC grade) to form a 1 mM spreading solution. Water (resistance 18 MΩ cm) purified in a Milli-Q system (Millipore) was used for preparing the aqueous $CaCO_3$ solutions as the subphase. Calcium chloride tetrahydrate, sodium hydrogen carbonate and sodium chloride (all suprapure quality) were obtained from Merck, Germany. The aqueous 2 mM and 4 mM $CaCO_3$ solutions were prepared by mixing equal volumes of $NaHCO_3$ and $CaCl_2{\cdot}4\ H_2O$ solutions (4 and 8 mM l^{-1} in 0.1 M l^{-1} NaCl) at 20 °C.

Procedures The $CaCO_3$ solutions were poured into a custom built PTFE trough (74×10 cm^2) with a maximum working area of 590 cm^2 and two simultaneously moving barriers.

Monolayers were formed by spreading 180 µl of solutions of lipids or mixtures of these, respectively, in chloroform on subphases containing $CaCO_3$ solutions at 20 °C with a microsyringe. The surface pressure π was measured with a filter paper (Schleicher & Schüll 589) Wilhelmy balance and was kept constant after reaching $\pi = 15$ mN m^{-1} by a feedback loop. The speed of monolayer compression was 20.7 $cm^2 min^{-1}$. The formation of solid $CaCO_3$ in the head group region of monolayers at the air-solution interface was followed in situ using a modified Brewster angle microscope BAM 2 from Nanofilm Technologie, Göttingen, with a 514 nm Ar-Kr laser (Coherent Innova 70 Spectrum).

Results and discussion

Two-component monolayers

The two-component monolayers on the subphase containing $CaCO_3$ used in this study behave quite differently depending on the components and the molar mixing ratio, as illustrated by the surface pressure-area (π-A) isotherms (Fig. 1).

For comparison, the isotherms of the monolayers of the pure components are also shown. Two mixtures have been selected for each system, ODA/MOD and OSA/MOD, respectively. Since the most important parameter in the first approximation is the surface density of the active groups, the isotherms are plotted as surface pressure versus the area per COOH group (except for MOD, area per molecule). The aqueous subphases were different in the two sets: 2 mM $CaCO_3$ for monolayers with ODA, and 4 mM $CaCO_3$ for monolayers with OSA. In the following, the behaviour of ODA:MOD = 3:2 will be compared to that of OSA:MOD = 1:2, and ODA:MOD = 9:11 with that of OSA:MOD = 1:3. At the surface pressure of 15 mN m^{-1} (horizontal dotted line in Fig. 1), these pairs have nearly the same area per COOH group and corresponding surface densities of the active groups (Table 1).

The shape of the π-A isotherms is quite different in the two systems. For the ODA mixtures, the surface pressure rises abruptly and quite steeply upon compression. At $\pi = 15$ mN m^{-1}, the observed area per COOH group coincides very well with that calculated

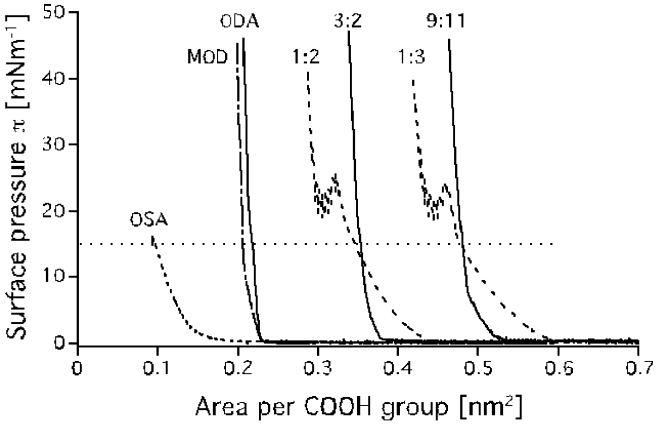

Fig. 1 Characterisation of monolayers at the air–solution interface by surface pressure (π)-area (A) isotherms. Area A plotted as area per COOH group [monolayers with octadecanoic acid (*ODA*) and octadecyl succinic acid (*OSA*), respectively] or area per molecule [methyl octadecanoate (*MOD*), *dash-dotted curve*]. *Full lines* Monolayers of ODA, ODA:MOD = 3:2, and ODA:MOD = 9:11; *dashed lines* OSA, OSA:MOD = 1:2, and ODA:MOD = 1:3; molar mixing ratios indicated at the *curves*; *horizontal dotted line* represents $\pi = 15$ mN m^{-1}. Subphase: $CaCO_3$, 2 mM (ODA monolayers) and 4 mM (OSA monolayers), respectively; 20 °C

Table 1 Monolayer parameters. Area per COOH group, A_{COOH}, (area per molecule for MOD) of monolayers at the surface of aqueous solutions of $CaCO_3$, at concentrations of 2 mM (monolayers with ODA) and 4 mM (monolayers with OSA, and of pure MOD), respectively. Parameters σ, t_0, and a of least squares fits of Eq. 1 to the observed time dependences of the area fraction of bright domains, f_{domain} (Fig. 3)

	A_{COOH}(nm^2)	A_{calc}(nm^2)	σ(s)	t_0 (s)	a
MOD	0.207	–	–	–	–
ODA	0.218	–	–	–	–
ODA:MOD = 3:2	0.353	0.356	380	2530	1[a]
ODA:MOD = 9:11	0.480	0.471	5552	15100	1[a]
OSA	0.097	–	–	–	–
OSA:MOD = 1:2	0.345	0.304	800*	1800*	0.433
OSA:MOD = 1:3	0.478	0.407	800*	1800*	0.179

*Parameter fixed

from the areas of the components indicating ideal behaviour (Table 1). This may be interpreted as a homogeneous distribution of the active groups in the inert matrix. The OSA mixtures, in contrast, show a smooth increase and a phase transition at a surface pressure of about 24 mN m^{-1}. The isotherm of OSA:MOD = 1:3 closely resembles that of OSA:MOD = 1:2, except for the displacement to larger area per COOH group (due to a larger fraction of the inert matrix). Such a behaviour is often taken as an indication of phase separation in the monolayer with the collapse of one phase occurring at the same surface pressure independent of the mixing ratio [16]. Therefore, the phase transition may be due to the collapse of a separate phase of OSA, since the monolayer of pure OSA is rather unstable. Alternatively, OSA might be stabilised (since the surface pressure of the phase transition is somewhat higher than the collapse pressure of OSA, $\pi_{collapse} \approx 18$ mN m^{-1}) by forming a phase of an association with MOD. The area per COOH at $\pi = 15$ mN m^{-1} observed for the two-component monolayers is larger than that calculated from the areas of the components (Table 1).

Brewster angle microscopy

BAM images of the two-component monolayers taken at different times t after starting the compression (first images recorded when the surface pressure π has reached 15 mN m^{-1}) clearly show the formation and growth of bright domains (Fig. 2).

At $\pi = 15$ mN m^{-1}, the monolayers ODA:MOD = 3:2 and OSA:MOD = 1:2 have the same average surface density of COOH groups initialising the formation of solid $CaCO_3$ at the interface (Fig. 1). However, a striking difference is seen in the images at $t \approx 1800$ s: many more bright domains indicating the ultra thin layer of $CaCO_3$ in contact with the monolayer head groups, are observed for OSA:MOD = 1:2 (Fig. 2b, $t = 1764$ s) than for ODA:MOD = 3:2 (Fig. 2a, $t = 1883$ s). Further, the time evolution differs dramatically for the two monolayers compared here. The area fraction covered with bright domains at $t \approx 2750$ s obviously is much larger for the monolayer with ODA (Fig. 2c, $t = 2733$ s) than with OSA (Fig. 2d, $t = 2765$ s).

Growth model for $CaCO_3$ domains

We have adapted to our needs a growth model used in the determination of heterogeneous nucleation rates [17]. A Gaussian size distribution of the bright domains of $CaCO_3$ in contact with the monolayer head groups is assumed. As the distribution shifts with time in size and thickness of the ultra thin layer, the domains become visible in the BAM exceeding a fixed brightness level. The time dependence of the area fraction f_{domain} of bright domains in the monolayer then is the integral of the Gaussian distribution, described as

$$f_{domain} = \frac{a}{2}\left(1 + \mathrm{erf}\left(\frac{t - t_0}{\sigma\sqrt{2}}\right)\right) \quad (1)$$

The parameter a represents the amplitude (limiting value of f_{domain} for $t \to \infty$), 2σ the half width of the Gaussian distribution, and t_0 the offset time of the distribution. With this type of dependence least squares fits to the results of the image evaluation have been performed (Fig. 3, solid lines) assuming a behaviour of the monolayers with ODA different from that with OSA. In case of the ODA monolayers, the amplitude value has been set to $a = 1$, and the two other parameters σ and t_0 have been obtained from the fit. All fit parameters are listed in Table 1. For fitting the curves to the data of ODA monolayers, the parameters $\sigma = 800$ s and $t_0 = 1800$ s have been set, and the amplitude a only was determined by fitting. This approach implies that in the case of ODA with homogeneously distributed active sites, the whole surface will eventually be covered with $CaCO_3$, although nucleation and growth may be too slow to observe this process within reasonable times. In contrast, the active sites are clustered in monolayers containing OSA due to

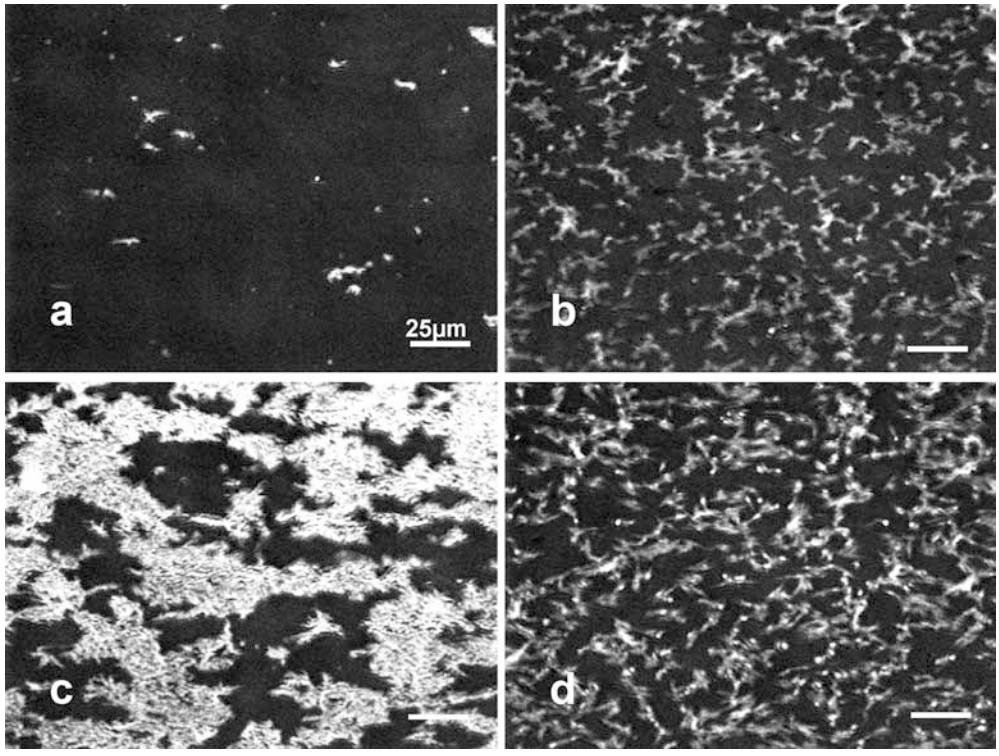

Fig. 2a–d Observation of $CaCO_3$ formation by Brewster angle microscopy. BAM images of monolayers on top of $CaCO_3$ solutions (2 mM for ODA:MOD = 3:2 and 4 mM for OSA:MOD = 1:2) taken at different times t.
a ODA:MOD = 3:2, t = 1883 s.
b OSA:MOD = 1:2, t = 1764 s.
c ODA:MOD = 3:2, t = 2733 s.
d OSA:MOD = 1:2, t = 2769 s.
Images taken at constant monolayer area (π = 15 mN m^{-1}); 20 °C

phase separation, and fast formation of $CaCO_3$ is observed even for small molar fractions of the active component as compared to monolayers containing ODA. Since no $CaCO_3$ is formed underneath the fraction of the monolayer with MOD, the amplitude in the time dependence varies with the molar fraction of the active component OSA.

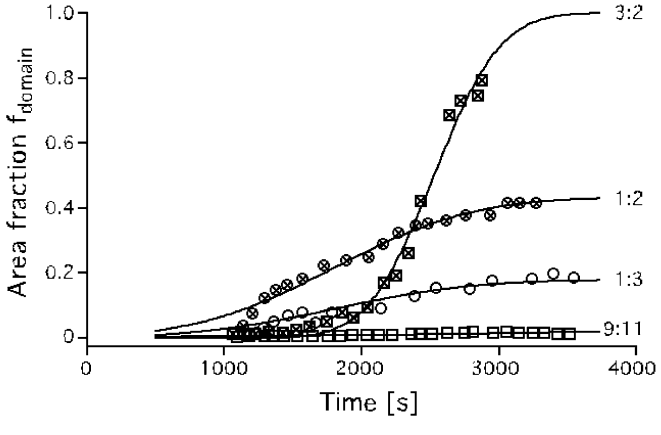

Fig. 3 Kinetics of $CaCO_3$ formation at two-component monolayers. Area fraction f_{domain} of bright domains determined from BAM images as function of time t for the monolayers ODA:MOD = 3:2 and 9:11 (*squares*), and OSA:MOD = 1:2 and 1:3 (*circles*), respectively as indicated; the *full curves* are least squares fits of Eq. 1 to the experimental data with the parameters listed in Table 1. Images taken at constant monolayer area (π = 15 mN m^{-1}); 20 °C

The series of images has been evaluated by determining the area fraction f_{domain} of domains exceeding a limiting brightness value. The results clearly indicate the fundamentally different behaviours of the monolayers ODA:MOD = 3:2 and OSA:MOD = 1:2, respectively; concerning kinetics of formation and area fraction of the bright domains extrapolated to very long times (Fig. 3). This becomes more evident by regarding the second pair of two-component monolayers, again with the same average surface density of active groups at π = 15 mN m^{-1}, i.e. ODA:MOD = 9:11 and OSA:MOD = 1:3 (Fig. 1). From the BAM images (not shown here), the time evolution of the area fraction of domains exceeding the limiting brightness level has been determined. Again, the two monolayers show a strikingly different behaviour (Fig. 3). Whereas domain formation is hardly visible with ODA, bright domains form rather rapidly at the monolayer with OSA, reaching a limiting value smaller than in the case of OSA:MOD = 1:2 after time $t \approx 3500$ s. Since the physical natures of the groups initialising the formation of solid $CaCO_3$ and of the inactive matrix are identical in both systems, the reason for the dramatically different behaviour of ODA containing monolayers as compared to monolayers with OSA has to be the different distribution of the active groups in the matrix.

To conclude, the formation of $CaCO_3$ in the head group region of insoluble two-component model monolayers at the solution-air interface has been observed by Brewster angle microscopy. Two pairs of

monolayers with the same average surface density of COOH groups have been compared. According to the surface pressure-area isotherms, the active component octadecanoic acid is homogeneously distributed in the inert matrix, whereas a phase separation of active component and matrix occurs in monolayers with octadecyl succinic acid as active component. The striking differences in kinetics and extent of $CaCO_3$ formation observed in these systems, therefore, have to be attributed to the different distributions of the active groups as evidenced by the surface pressure-area isotherms. This fact demonstrates the dominant role of the lateral distribution of active sites in the process of biomineralisation at interfaces. In particular, the observations suggest that a minimum number of active groups (a critical cluster) is required to act as nucleation site for the formation of solid $CaCO_3$.

Further investigations using in situ synchrotron X-ray scattering will help to improve our understanding on the influence of the active sites distribution on the $CaCO_3$ formation, as well as to determine the specific $CaCO_3$ polymorph phases.

Acknowledgements This work has been supported by the Deutsche Forschungsgemeinschaft (Mo 156/5). We thank the Fonds der Chemischen Industrie, Germany, for financial support.

References

1. Weiner S, Traub W, Lowenstam HA (1983) Organic matrix in calcified exoskeletons. In: Westbroek P, de Jong EW (eds) Biomineralization and biological metal accumulation. Reidel, Dordrecht, pp 205–224
2. Weiner S, Addadi L, Wagner HD (2000) Mater Sci Eng C 11:1
3. Lowenstam HA, Weiner S (1989) On biomineralization, Oxford University Press, New York
4. Simkiss K, Wilbur K (1989) Biomineralization: cell biology and mineral deposition. Academic, San Diego
5. Neu TR, Lawrence JR (1999) In situ characterization of extracellular polymeric substances (EPS) in biofilm systems. In: Wingender J, Neu TR, Flemming HC (eds) Microbial extracellular polymeric substances, Springer, Berlin Heidelberg New York, pp 21–47
6. Heywood BR, Mann S (1994) Adv Mater 6:9
7. Litvin AL, Valiyaveettil S, Kaplan DL, Mann S (1997) Adv Mater 9:124
8. Weissbuch I, Majewski J, Kjaer K, Als-Nielsen J, Lahav M, Leiserowitz L (1993) J Phys Chem 97:12848
9. Kuzmenko I, Rapaport H, Kjaer K, Als-Nielsen J, Weissbuch I, Lahav M, Leiserowitz L (2001) Chem Rev 101:1659
10. Hénon S, Meunier J (1991) Rev Sci Instr 62:936
11. Hönig D, Möbius D (1991) J Phys Chem 95:4590
12. Hönig D, Overbeck GA, Möbius D (1992) Adv Mater 4:419
13. Edler KJ, Roser J, Mann S (2000) Chem Commun 9:773
14. Loste E, Diaz-Marti E, Zarbakhsh A, Meldrum FC (2003) Langmuir 19:2830
15. Hacke S (2001) Brewsterwinkel-Mikroskopie zur Untersuchung der Kristallisation von Calcium-carbonaten an Modell-Monofilmen an der Grenzfläche Wasser/Luft. PhD Thesis, University of Göttingen
16. Adamson AW (1976) Physical chemistry of surfaces, 3rd edn. Wiley, New York
17. Schubert H, Mersmann A (1996) Trans I Chem E 74 A:821